An optimized tracer-based approach for estimating organic carbon emissions from biomass burning in Ulaanbaatar, Mongolia

Jayant Nirmalkar[1], Tsatsral Batmunkh[2], Jinsang Jung[1,*]

[1]Center for Gas Analysis, Korea Research Institute of Standards and Science (KRISS), Daejeon 34113, Republic of Korea

[2]Department of Green Development Policy and Planning, Ministry of Environment and Tourism, UIaanbaatar-15160, Mongolia

Correspondence to: Jinsang Jung (jsjung@kriss.re.kr)

Abstract

The impact of biomass burning (BB) on atmospheric particulate matter of <2.5 μm diameter ($PM_{2.5}$) at Ulaanbaatar, Mongolia, was investigated using an optimized tracer-based approach during winter and spring, 2017. Integrated 24 h $PM_{2.5}$ samples were collected on quartz fiber filters using a 30 L min^{-1} air sampler at an urban site in Ulaanbaatar. The aerosol samples were analyzed for organic carbon (OC) and elemental carbon (EC), anhydrosugars (levoglucosan, mannosan, and galactosan), and water-soluble ions. OC was found as the predominant species, contributing 64% and 56% to the quantified aerosol components in $PM_{2.5}$ in winter and spring, respectively. BB was identified as a major source of $PM_{2.5}$, followed by dust and secondary aerosols. Levoglucosan/mannosan and levoglucosan/K^+ ratios indicate that BB in Ulaanbaatar was mainly originated from burning of softwood. Because of the large uncertainty associated with quantitative estimation of OC emitted from BB (OC_{BB}), a novel approach was developed to optimize the OC/levoglucosan ratio for estimating OC_{BB}. The optimum OC/levoglucosan ratio in Ulaanbaatar was obtained by regression analysis between $OC_{non\text{-}BB}$ (OC_{total}–OC_{BB}) and levoglucosan concentrations that gives the lowest coefficient of determination (R^2) and slope. The optimum OC/levoglucosan ratio was found to be 27.6 and 18.0 for winter and spring, respectively, and these values were applied in quantifying OC_{BB}. It was found that 68% and 63% of the OC were emitted from BB during winter and spring, respectively. This novel approach can also be applied to other study sites to quantify OC_{BB} using their own chemical measurements. In addition to OC_{BB}, sources of $OC_{non\text{-}BB}$ were also investigated through multivariate correlation analysis. It was found that $OC_{non\text{-}BB}$ was originated mainly from coal burning, vehicles, and vegetative emissions.

***Keywords*:** Source identification, Biomass burning, Optimized organic-carbon/levoglucosan ratio

1. Introduction

Organic aerosol (OA) contributes a significant fraction (10%−90%) of atmospheric particulate matter (PM), which can affect human health and air quality (Jimenez et al., 2009; Maenhaut et al., 2011; Fu et al., 2012; Allan et al., 2014; Chen et al., 2018). An understanding of the sources of PM is highly relevant for air-quality remediation. Biomass burning (BB) is a major source of organic carbon (OC) in $PM_{2.5}$ (PM with aerodynamic diameter ≤2.5 μm) and it may become more significant in the future as air-quality regulations restrict other anthropogenic emissions (Davy et al., 2011; Allan et al., 2014; Sullivan et al., 2019). Coal combustion, thermal power plants, and traffic emissions also make potential contributions to the OC content of PM (Watson et al., 2001a, b; Pei et al., 2016; Deshmukh et al., 2019; Haque et al., 2019), modifying PM characteristics such as hygroscopicity, light-attenuating properties, and health impacts (Jung et al., 2009; Sullivan et al., 2019). Previous studies have observed that the toxicity of $PM_{2.5}$ increases with the oxidation potential of BB species because of the water-soluble fraction of OC (Verma et al., 2014).

Previous studies have identified and quantified OC emitted from BB (OC_{BB}) using the BB tracers (levoglucosan, mannosan, galactosan, and K^+). Levoglucosan is produced from the pyrolysis of cellulose at temperatures of >300°C (Simoneit et al., 1999; Claeys et al., 2010; Maenhaut et al., 2011; Nirmalkar et al., 2015; Achad et al., 2018); and two isomers of levoglucosan, mannosan and galactosan are produced by the burning of hemicellulose (Reche et al., 2012). The atmospheric concentration of levoglucosan is higher than that of the two isomers because of the lower content of hemicellulose (20%−30%, dry weight) than cellulose (40%−50%) in softwood and hardwood (Reche et al., 2012; Sharma et al., 2015). Water-soluble K^+ can also be used

as a BB tracer (Pio et al., 2008; Cheng et al., 2013; Nirmalkar et al., 2015; Chen et al., 2018; Chantara et al., 2019). The proportion of these BB tracers in PM depends on various factors such as the type of biomass (softwood, hardwood, crop, grass, etc.), where it is burnt (traditional stoves, fireplaces, field burning, burning in closed chambers, etc.), the type of burning (smoldering, flaming, etc.), and the burning season (Fu et al., 2012; Cheng et al., 2013; Jung et al., 2014). Levoglucosan/mannosan, levoglucosan/K^+, and OC/levoglucosan ratios were used to identify major biomass types and quantify OC_{BB} (Reche et al., 2012; Cheng et al., 2013; Jung et al., 2014; Chen et al., 2018). However, OC/levoglucosan ratios are quite variable even with the same type of BB because of variations in burning type, place, and season (Cheng et al., 2013; Thepnuan et al., 2019 and references therein). It is therefore essential to optimize the OC/levoglucosan ratio to better estimate OC_{BB}.

Ulaanbaatar, with a population of about 1 million, is an atmospheric pollution 'hotspot' because of its topography, being situated in the Tuul river valley and surrounded by the Khentei mountains, with a high elevation (1300 m−1949 m above sea level) and large variations in temperature (–28°C to +16°C) and relative humidity (17.7%–72.7%; Table 1; Batmunkh et al., 2013; Jung et al., 2014). As the world's coldest capital city during winter, it requires additional fuel for space heating. The topography and low-temperature conditions cause an increase in PM concentrations, which are exacerbated by low wind speeds and atmospheric temperature inversions (Jung et al., 2010).

Half of the residents in Ulaanbaatar lives in 160,000 Gers (traditional Mongolian dwellings) (Guttikunda and Jawahar, 2014). Biomass is used as fuel for cooking and heating in many of low-income Gers at Ulaanbaatar. The common tree species in

Mongolia are larch, pine, cedar, spruce, birch; these are mostly softwood (http://www.fao.org/3/w8302e/w8302e05.htm; http://www.fao.org/3/a-am616e.pdf, excess date 17-12-2019). Each Ger burns an average of 3 m^3 of wood per year (Guttikunda, 2008; Zhamsueva et al., 2018). Organic carbon (OC) has severe effects on human health and global climate change (Sun et al., 2019). But there are very few estimates of OC emitted from biomass burning (OC_{BB}) in Ulaanbaatar. Few studies have investigated the chemical characteristics of aerosol in Ulaanbaatar (Jung et al., 2010; Davy et al., 2011; Batmunkh et al., 2013), with none examining the contribution of OC_{BB} and type of biomass. Therefore, this study estimated appropriate concentration of OC_{BB} and identified the type of biomass at Ulaanbaatar, Mongolia.

In this study, we quantified the BB tracers levoglucosan, mannosan, galactosan, K^+, and other chemical species. Potential sources of $PM_{2.5}$ were identified by principal component analysis (PCA), with levoglucosan/K^+ and levoglucosan/mannosan ratios being used to identify major biomass types. OC_{BB} can be quantified from OC/levoglucosan ratios and levoglucosan concentrations in PM. However, uncertainties of OC_{BB} are high because OC/levoglucosan ratios can vary depending on fuel type, burning conditions, and burning place (Duan et al., 2004; Cheng et al., 2013; Jung et al., 2014). Therefore, it is required to determine the most suitable OC/levoglucosan ratio of BB emissions for estimating appropriate concentration of OC_{BB}. Here, for the first time, optimized OC/levoglucosan ratios were investigated for estimating concentrations of OC_{BB} during winter and spring. $OC_{non\text{-}BB}$ sources were also investigated using multivariate correlation analysis with ions and elemental carbon (EC).

2. Methods

2.1 Sampling site and aerosol sampling

Aerosol sampling was carried out in Ulaanbaatar during the winter (17 January to 03 February) and spring (17 April to 4 May) of 2017, with 24 h periods commencing daily at 11:00 local time. An aerosol sampler was installed on the rooftop of the National Agency for Meteorology and Environmental Monitoring station in Ulaanbaatar (47°92' N, 106°90' E, Fig. 1), 10 m above ground level. The sampling site was located at 8 km–10 km far from two coal based thermal power plants to the west (Chung and Chon, 2014). $PM_{2.5}$ samples were collected on 47 mm diameter quartz fiber filters (Pall-Life Sciences, USA) using an aerosol sampler (Murata Keisokuki Service, Japan) at a flow rate of 30 L min^{-1}. Field blank filter was collected during winter (n=1) and spring (n=1). The quartz fiber filter was loaded in the sampler for 5 minutes without operating a pump. The concentration of all chemical analytes has been corrected using blank filters concentration. Sampled filters were wrapped in aluminum foil and heated at 550°C for 12 h to remove adsorbed impurities before use and stored at –20°C before and after sampling.

2.2 Filter analysis

A one-fourth part of each quartz fiber filter sample was extracted in 10 mL ultrapure water (resistivity 18.2 MΩ, total OC content < 1 ppb,) under ultrasonication for 30 min. The water extract was then filtered using a syringe filter (Millipore, Millex−GV, 0.45μm) and stored at 4°C pending analysis. Water-soluble cations (K^+, Na^+, Ca^{2+}, Mg^{2+}, and NH_4^+) were quantified by an ion chromatograph (Dionex ICS 5000, Thermo Fisher Scientific, USA). Water-soluble cations were separated using an IonPac CS−12A column (Thermo Fisher Scientific, USA) with 20 mM methanesulfonic

136 acid as eluent at a flow rate of 1.0 mL min^{-1}. Water-soluble anions (Cl^-, NO_3^-, and
137 SO_4^{2-}) were separated using an IonPac AS−15 column (Thermo Fisher Scientific, USA)
138 with 40 mM KOH as eluent at a flow rate of 1.2 mL min^{-1}. The detection limits for
139 major inorganic ions based on 3σ of blanks were 0.01 μg m^{-3}, 0.01 μg m^{-3}, and 0.03 μg
140 m^{-3} for NO_3^-, SO_4^{2-}, and NH_4^+, respectively.

141 Levoglucosan, mannosan, and galactosan were measured by a high-performance
142 anion-exchange chromatograph (Dionex, ICS−5000, Thermo Fisher Scientific, USA)
143 with pulsed amperometric detection involving an electrochemical detector with a gold
144 working electrode. Details of the method are given elsewhere (Jung et al., 2014). In
145 brief, separation involved a CarboPak MA1 (4 × 250 mm, Thermo Fisher Scientific,
146 USA) analytical column and NaOH eluent (360 mM, 0.4 mL min^{-1}). Limits of detection
147 were 3.0 ng m^{-3}, 0.7 ng m^{-3}, and 1.0 ng m^{-3} for levoglucosan, mannosan, and galactosan,
148 respectively.

149 Aerosol samples were analyzed for OC and EC using a thermal optical OC/EC
150 analyzer (Sunset Laboratory Inc. Forest Grove, OR, USA) with laser transmittance-
151 based correction of pyrolysis. Details of the analyzer and quality-control parameters are
152 reported elsewhere (Jung et al., 2014). In brief, 1.5 cm^2 punch samples of the quartz
153 fiber filter were placed in a quartz dish inside the thermal desorption oven of the
154 analyzer. OC and EC were quantified using a temperature program developed by the US
155 National Institute for Occupational Safety and Health (NIOSH) in an inert atmosphere
156 (100% He) and in an oxidizing atmosphere (98% He + 2% O_2), respectively. Detection
157 limits of OC and EC were 0.04 and 0.01 μg C m^{-3}, and analytical uncertainties of them
158 were 1.3% and 3.7%, respectively.
159

160 2.3. Conditional Probability Function

161 The Conditional Probability Function (CPF) calculates the probability that a source
162 is located within a particular wind direction sector, ΔΘ:

163 $$CPF = \frac{m_{\Delta\Theta}}{n_{\Delta\Theta}}$$

164 where $n_{\Delta\Theta}$ is the number of times that the wind passed through direction sector ΔΘ,
165 and $m_{\Delta\Theta}$ is the number of times that the source contribution peaked while the wind
166 passed through sector ΔΘ (Ashbaugh et al., 1985). To use CPF with the Ulaanbaatar
167 data, the 24 h averaged source contribution data have been applied to all 1 h wind
168 direction averages recorded at the site for each date. The angular interval ΔΘ was set at
169 10°. To calculate $m_{\Delta\Theta}$, the 75th percentiles of source contribution concentrations were
170 counted. CPF is useful in determining the direction of a source from a receptor site;
171 however, it cannot determine the actual location of the source.

172

173 2.4 Principal component analysis

174 In order to identify the source groupings of chemical species in $PM_{2.5}$, principal
175 component analysis (PCA) was applied. PCA is done using a commercially available
176 software package (SPSS, version 10.0). PCA applies projection dimension reduction
177 methods, converting several concentrations sets into significant sets of columns
178 (principal components, PCs) without damaging the original data. PCA is a widely used
179 statistical technique to quantitatively identify a small number of independent factors
180 among the species concentrations, which can explain the variance of the data, by using
181 the eigenvector decomposition of a matrix of pair-wise correlations. PCA with varimax
182 rotation and retention of principal components having eigenvalues >1.0 was used to

identify major species associated with different sources. It was widely used for identification of pollution sources in the atmosphere (Fang et al., 2003, Nirmalkar et al., 2015).

3. Results and Discussion

3.1 Chemical characteristics of $PM_{2.5}$ and source identification

Mass concentrations of carbonaceous aerosol, BB tracers, and water-soluble ions in $PM_{2.5}$ samples collected at Ulaanbaatar during winter and spring of 2017 are summarized in Table 1. OC contributed 64 ± 5.1% and 56 ± 6.0% of the quantified aerosol components in $PM_{2.5}$ in winter and spring, respectively (Table 1). Average concentrations of OC during winter were five times those obtained in spring (Fig. 2). Previously, OC has been observed as major component in $PM_{2.5}$ in Ulaanbaatar during winter period (Jung et al., 2010; Batmunkh et al., 2013). This may be attributed to additional BB emission for home heating, and temperature inversions with low wind speeds (average wind speed of 1.43 ± 0.73 m s^{-1}; Table 1 and Fig. 3a). OC concentrations decreased with increasing wind speed during winter (Fig. 3a) and spring (Fig. 3b), over all air temperature ranges. The inverse relationship between OC and wind speed during winter (Fig. 3a) and spring (Fig. 3b) suggests a predominance of local sources, with higher wind speeds flushing air pollutants out of the area whereas low wind speeds allow them to accumulate (Khan et al., 2010; Wang et al., 2018).

Average concentration of EC during winter (1.71 ± 0.58 μg m^{-3}) was higher than that in spring (1.11 ± 0.42 μg m^{-3}) (Table 1), consistent with general urban observations in cities of China (Ji et al., 2016) and India (Panda et al., 2016). During both winter and spring, EC concentrations at the study site were lower and having different trends

compared to those observed in a suburban site (2.3 ± 1.0 μg m^{-3} and 3.1 ± 1.5 μg m^{-3}, respectively) and an urban site (2.3 ± 1.0 μg m^{-3} and 3.3 ± 1.2 μg m^{-3}, respectively) in Shanghai, China (Feng et al., 2009).

The potential source direction of EC during winter and spring was west as shown in Fig. 5; this can be explained by the influence of emission from thermal power plants. Correlation of EC was strong with Ca^{2+} during spring as shown in Fig. 4. CPF analysis suggested that potential source direction of EC and Ca^{2+} was similar (Fig. 5). High abundances of Ca^{2+} and EC is observed from stack emission of coal fired thermal power plants (Pei et al., 2016; Zhang et al., 2015). Thus, EC and Ca^{2+} in Ulaanbaatar might be strongly related to emission from thermal power plants.

Daily concentrations of levoglucosan, mannosan and galactosan have similar trends during winter and spring (Fig. 2), possibly because of combustion of similar biomass fuels in both seasons. Changes in concentrations of these BB tracers might be attributed to changes in relative proportions of cellulose and hemicellulose in different biomass fuels (Zhu et al., 2015; Nirmalkar et al., 2015). Concentrations of anhydrosugars were four times higher in winter than in spring (Table 1) due to increased heating requirements in winter. The higher relative humidity (58.5%–72.7%) and lower temperature (–10.5°C to –27.8°C; Table 1) in winter can also contribute to longer atmospheric residence times due to increased levoglucosan stability (Lai et al., 2014). Higher concentrations of BB tracers in winter than spring have previously been observed in Beijing, China, (Liang et al., 2016) and were attributed to meteorological conditions similar to those of Ulaanbaatar. Average K^+ concentration (0.08±0.05 μg m^{-3}) in this study is significantly lower than the K (0.32 μg m^{-3}) observed in Ulaanbaatar during 2004-2008 (Davy et al., 2011).

Among water-soluble ions, SO_4^{2-} (9.7 ± 3.4 μg m^{-3}) was the most dominant $PM_{2.5}$ species during winter, followed by NH_4^+ (6.2 ± 2.4 μg m^{-3}) and NO_3^- (4.2 ± 1.7 μg m^{-3}), whereas SO_4^{2-} (1.9 ± 0.5 μg m^{-3}) was the dominant species during spring, followed by Ca^{2+} (0.9 ± 0.4 μg m^{-3}) and NH_4^+ (0.7 ± 0.3 μg m^{-3}). The total SO_4^{2-} + NH_4^+ + NO_3^- content accounted for 27% and 23% of the total measured chemical species during winter and spring, respectively (Fig. 2 and Table 1). SO_4^{2-} is the most prevalent water-soluble ion in $PM_{2.5}$ in Wuhan, Guangzhou, and Tianjin (China) due to industrial emissions and coal burning (Gu et al., 2011; Tao et al., 2014; Huang et al., 2016; Pei et al., 2016). This suggests that the higher SO_4^{2-} concentration in Ulaanbaatar may be attributable to emissions from the three major coal-fired thermal power plants near the study site.

The atmospheric concentrations of OC (11–17 μg m^{-3}) and levoglucosan (0.46–0.73 μg m^{-3}) were higher for samples collected during 27–30 April 2017 than on almost all remaining days in spring (Fig. 2b). Backward atmospheric trajectories based on the Hybrid Single-Particle Lagrangian Integrated Trajectory (HYSPLIT) model provided by the US National Oceanic and Atmospheric Administration (NOAA) Air Resources Laboratory (ARL) indicate that during those days' air masses originated from a region where a significant number of fires were detected [US Fire Information for Resource Management System (FIRMS); National Aeronautics and Space Administration (NASA); Fig. 6a, b)]. Thus, the elevated OC and levoglucosan concentrations during 27–30 April might be influenced by long-range transport of BB from north of Mongolia.

3.2 Principal Component Analysis

Principal component analysis (PCA) is a useful tool for reducing the dimensionality

of large aerosol datasets to principal components using varimax rotation for source identification (Cao et al., 2005; Lin et al., 2018; Nirmalkar et al., 2019). Four principal components (PCs) in winter and three in spring were identified with eigenvalues >1 after varimax rotation explaining 96% and 92%, respectively, of the total variance (Tables 2 and 3). The PCs were categorized on the basis of loadings of chemical components as follows. In winter, PC1 includes BB characterized by high loadings of levoglucosan, mannosan, and galactosan; PC2 includes dust characterized by Ca^{2+} and Mg^{2+} content; PC3 includes secondary formation characterized by SO_4^{2-}, NO_3^-, and NH_4^+ content; and PC4 includes fossil fuel combustion characterized by EC. In spring, PC1 includes BB (levoglucosan, mannosan, and galactosan); PC2 includes dust (Ca^{2+} and Mg^{2+}) and fossil fuel combustion (EC); and PC3 includes secondary formation (SO_4^{2-}, NO_3^-, and NH_4^+). The PCA results show that the chemical components of $PM_{2.5}$ in Ulaanbaatar were mainly affected by BB during winter and spring. Further, OC was primarily influenced by BB because it correlated well with the total variance of PC1 during winter (0.82; Table 2) and spring (0.77; Table 3).

3.3 Relationship among BB tracers

The correlations among the three BB tracers levoglucosan, mannosan, and galactosan are shown in Fig. 7a (winter) and 7b (spring). The correlations between levoglucosan and mannosan and between levoglucosan and galactosan are strong during winter ($R^2 = 0.99$ for both pairs) and spring ($R^2 = 0.95$ and 0.83, respectively; Fig. 7a, b). Concentrations of levoglucosan and OC are strongly correlated during both winter ($R^2 = 0.78$) and spring ($R^2 = 0.86$; Fig. 8a), suggesting that a major fraction of OC might be originated from BB in Ulaanbaatar. The similar strong correlation and steep slope

observed in OC–levoglucosan plots for PM collected in Chiang Mai Province (Thailand) and Daejeon (Korea) were attributed mainly to BB (Jung et al., 2014; Thepnuan et al., 2019).

Fine mode K^+ is considered as biomass burning tracer in previous studies (Louie et al., 2005; Deshmukh et al., 2011; Cheng et al., 2013). The moderate correlation between levoglucosan and K^+ concentrations (R^2 = 0.68) in winter indicates that they are produced from similar sources (Fig. 8b), with BB contributing most of the K^+. However, the correlation between levoglucosan and K^+ was weak in spring (R^2 = 0.49; Fig. 8b). Because K^+ is typically emitted at a higher mass fraction in flaming phase combustion compared to smoldering (Lee et al., 2010), smoldering combustion tends to have higher levoglucosan/K^+ emission ratio compared to flaming combustion (Schkolnik et al., 2005; Gao et al., 2003). High levoglucosan/K^+ ratio was observed during winter (8.92) compared to spring (4.21) in this site. Thus, week correlation between levoglucosan and K^+ concentrations at Ulaanbaatar in spring can be explained by mixed burning condition such as smoldering and flaming.

OC and K^+ concentrations correlated well during winter (R^2 = 0.79; Fig. 9a) and spring (R^2 = 0.73; Fig. 9b), suggesting that they might be originated from similar sources. Because most of the aerosol particles emitted from BB belong to $PM_{2.5}$, the correlation between OC and K^+ as well as levoglucosan suggests that BB is one of the potential sources of OC in winter and spring. Because biomass fuel is burned in traditional stoves with no pollution control devices in Ulaanbaatar (Batmunkh et al., 2013), soil and ash particles are entrained in convective processes and uplifted in the atmosphere together with smoke particles (Deshmukh et al., 2011; Nirmalkar et al., 2019).

303

304 3.4 Tracing the source of BB aerosol

305 OC is a major contributor of the quantified aerosol components in $PM_{2.5}$ in
306 Ulaanbaatar during spring and winter (Table 1). To quantify the OC_{BB}, it is necessary to
307 identify the BB fuel type. Several investigators used levoglucosan/mannosan and
308 levoglucosan/K^+ ratios to identify BB fuel types (Puxbaum et al., 2007; Cheng et al.,
309 2013; Jung et al., 2014; Chen et al., 2018; Thepnuan et al., 2019).

310 The levoglucosan/mannosan ratio is source-specific and can be used to identify BB
311 fuel types due to the unique cellulose and hemicellulose compositions of different
312 biomass fuels (Zhang et al., 2007; Cheng et al., 2013). A previous study suggested that
313 the levoglucosan/mannosan ratio is strongly dependent on wood type, rather than on the
314 site where the wood is grown (Cheng et al., 2013). Therefore, the
315 levoglucosan/mannosan ratio was used to trace the type of wood burnt during winter
316 and spring for indoor heating and cooking purposes. Previous studies have used
317 levoglucosan/mannosan ratios to investigate the BB fuel types (Cheng et al., 2013; Jung
318 et al., 2014).

319 However, the levoglucosan/mannosan ratio can't distinguish crop residuals (29 ± 15)
320 (Sheesley et al., 2003, Sullivan et al., 2008, Engling et al., 2009, Oanh et al., 2011) and
321 hardwood (28 ± 28) (Fine et al. 2001, 2002, 2004a, b; Engling et al., 2006; Schmidl et
322 al., 2008; Bari et al., 2009; Goncalves et al., 2010) due to the overlap of ratios between
323 these fuel types (Cheng et al., 2013; Fine et al. 2001, 2002, 2004a, b; Engling et al.,
324 2006). However, levoglucosan/K^+ ratio can distinguish between the two groups (Jung et
325 al., 2014, Chen et al., 2018). Both levoglucosan/mannosan and levoglucosan/K^+ ratios
326 are therefore useful in distinguishing various types of fuel (Cheng et al., 2013; Puxbaum

et al., 2007).

A levoglucosan/mannosan–levoglucosan/K^+ scatter plot based on results of the present and previous studies is shown in Fig. 10, using data from Schauer et al. (2001), Fine et al. (2001, 2002, 2004a, b), and Engling et al. (2006) for hardwood grown in the USA; Schauer et al. (2001), Hays et al. (2002), Fine et al. (2001, 2002, 2004a, b), and Engling et al. (2006) for US softwood; Schmidl et al. (2008), Bari et al. (2009) and Goncalves et al. (2010) for hardwood grown in Europe; Iinuma et al. (2007), Schmidl et al. (2008), and Goncalves et al. (2010) for European softwood; Engling et al. (2006) and Sullivan et al. (2008) for needles and duff found in the USA; Sullivan et al. (2008) for US grass; and from Sheesley et al. (2003), Sullivan et al. (2008), Engling et al. (2009) and Oanh et al. (2011) for Asian rice straw.

The average levoglucosan/mannosan ratio was 3.6 ± 0.2 (range: 3.4 − 4.1) in winter and 4.1 ± 1.0 (2.12 − 7.05) in spring, whereas the levoglucosan/K^+ ratio was 8.9 ± 1.8 (5.5 − 12.4) in winter and 4.2 ± 2.1 (0.58 – 7.49) in spring at the study site (Fig. 10), within the ranges reported for softwood burning sources (2.5 − 6.7 and 4.6 − 261, respectively) (Fine et al., 2001; Schauer et al., 2001; Fine et al., 2002, 2004a, b; Hays et al., 2002; Engling et al., 2006; Iinuma et al., 2007; Schmidl et al., 2008; Goncalves et al., 2010; Cheng et al., 2013). During winter and spring, the levoglucosan/K^+ and levoglucosan/mannosan ratios in Ulaanbaatar appeared in the softwood region (Fig. 10).

Therefore, softwood burning seems to be the major source of BB aerosol in Ulaanbaatar during both winter and spring, consistent with previously reported softwood-burning emissions from fireplaces of northern and southern regions of the USA (Fine et al., 2001, 2002), from household combustion in Zhengzhou, China (Chen et al., 2018), and from stove wood combustion in the mid-European region (Austria;

351 Schmidl et al., 2008).

352

353 3.5 Optimization of OC/levoglucosan ratio for estimating OC_{BB} emission

354 OC_{BB} was estimated by multiplying OC/levoglucosan ratio and levoglucosan
355 concentration. Previous studies have used the OC/levoglucosan ratio obtained from
356 sources of BB aerosol to estimate OC_{BB}. A ratio of 7.35 reported for burning of four
357 types of US hardwood (Fine et al., 2002) was used for estimating OC_{BB} at four
358 background sites in Europe (Puxbaum et al., 2007). Later, mean value of 11.2 of
359 OC/levoglucosan ratio derived from ratios ranged between 4.5 – 24.6 was used for
360 estimating OC_{BB} in the UK (Harrison et al., 2012). However, such estimates may not be
361 accurate as the OC/levoglucosan ratio is highly variable in BB emissions. For example,
362 the average OC/levoglucosan ratio from softwood burning (23.8) is much higher than
363 that of hardwood burning (7.35) (Fine et al., 2002; Schmidl et al., 2008), differences are
364 more than ten-fold among studies of softwood-burning OC/levoglucosan ratios (Fine et
365 al., 2002; Hays et al., 2002; Engling et al., 2006; Iinuma et al., 2007; Goncalves et al.,
366 2010). Combustion conditions may also significantly influence OC/levoglucosan ratios.
367 For example, the OC/levoglucosan ratio varied by a factor of about seven between
368 burning the same wood (Loblolly pine) in a fireplace (27.6; Fine et al., 2002) and in a
369 stove (3.4; Fine et al., 2004b). Therefore, it is necessary to optimize the
370 OC/levoglucosan ratio for use in estimating OC_{BB}.

371 This study has used an optimized OC/levoglucosan ratio to estimate precise
372 concentration of OC_{BB} for the Ulaanbaatar study site. We have used a range of different
373 OC/levoglucosan ratios obtained from previous literatures (Fig. 11) for regression
374 analysis with measured levoglucosan concentrations to estimate optimum

375 OC/levoglucosan ratio (Fig. 12a, b). First, candidate OC_{BB} (Fig. 11) in this study was
376 estimated from OC/levoglucosan ratios for softwood burning in a previous chamber
377 experiments (Cheng et al., 2013; Schauer et al., 2001; Hays et al., 2002; Fine et al.,
378 2001, 2002, 2004a, b; Engling et al., 2006; Iinuma et al., 2007; Schmidl et al., 2008;
379 Goncalves et al., 2010, Fig 11) and measured levoglucosan concentration at this site.
380 Second, $OC_{non\text{-}BB}$ concentration was calculated by subtracting OC_{BB} from corresponding
381 total OC. If calculated $OC_{non\text{-}BB}$ doesn't contain OC_{BB}, both regression slope and R^2
382 between $OC_{non\text{-}BB}$ versus levoglucosan will be close to zero. As shown in Fig. 12a and
383 12b, the lowest R^2 and regression slope were observed when OC/levoglucosan ratios of
384 27.6 and 18.0 in winter and spring, respectively. Thus, the optimized OC/levoglucosan
385 ratios for our site were determined to be 27.6 and 18.0 in winter and spring, respectively.
386 During winter higher optimum ratio of OC/levoglucosan might be due to
387 incomplete combustion during smoldering phenomena. As smoldering fires are
388 characterized by lower temperatures and thus have lower combustion efficiency, they
389 release more un-combusted condensable products, resulting in the production of more
390 unbroken organic compounds (Engling et al., 2006). Smoldering combustion generally
391 leads to increased emissions of volatile organic compounds (VOCs) and particulate
392 organic matter (OM) (Obrist et al., 2007). In contrast, the relatively lower optimum ratio
393 of OC/levoglucosan during spring might be due to the higher combustion efficiency
394 during flaming phenomena.
395 The OC_{BB} concentrations at the Ulaanbaatar study site were calculated from the
396 optimized OC/levoglucosan ratios (winter: 27.6 and spring: 18.0) and measured
397 levoglucosan concentrations. The OC_{BB} concentration was estimated to be 33.1 ± 11.9
398 μg C m^{-3} (range 16.0−58.5 μg C m^{-3}) and 5.64 ± 3.29 μg C m^{-3} (range 0.57−13.1 μg C

399 m^{-3}), accounting for 68% and 63% of the total OC in winter and spring, respectively
400 (Fig. 13). The average of previously published OC/levoglucosan ratios, 10.1 ± 7.9
401 (range 1.90 − 27.6), gives an estimated OC_{BB} concentration of 12.1 ± 4.4 μg C m^{-3}
402 (range 5.9−21.4 μg C m^{-3}) and 3.2 ± 1.8 μg C m^{-3} (0.32−7.34 μg C m^{-3}) in winter and
403 spring, respectively. Their values are 2.7 (winter) and 1.8 (spring) times lower than
404 values estimated using our optimized OC/levoglucosan ratio.

405 Our estimated contribution of OC_{BB} was higher than that in Daejeon, South Korea
406 (24%–68% of total OC, mean 45% ± 12%; Jung et al., 2014) and Beijing, China (50%
407 of total OC; Cheng et al., 2013), where BB aerosols are produced mainly by the burning
408 of crop residues. The contribution of OC_{BB} to total OC is 57% and 31% during heating
409 (average temperature 0.6°C) and non-heating (average temperature 14°C) seasons in
410 Krynica Zdroj, Poland (Klejnowski et al., 2017), significantly lower than that of
411 Ulaanbaatar during both winter (average temperature –21°C) and spring (average
412 temperature 6°C). Such high concentrations of OC_{BB} in Ulaanbaatar and Krynica Zdroj
413 are likely due to intense wood burning for heating during winter.

414

415 3.6 Tracing sources of $OC_{non\text{-}BB}$

416 High concentration of $OC_{non\text{-}BB}$ was found during winter compared to spring (Fig.
417 13). Elevated $OC_{non\text{-}BB}$ could be attributed to enhanced emission from combustions and
418 favorable meteorological conditions (cold temperatures and inversion conditions, etc.)
419 during the winter. There is strong correlation between $OC_{non\text{-}BB}$ and SO_4^{2-}, NH_4^+, and K^+
420 in winter and $OC_{non\text{-}BB}$ and NO_3^-, Na^+, K^+, Mg^{2+}, Ca^{2+}, and EC in spring (Table 4).
421 Residential combustion of coal emits significant amounts of OC, EC, and inorganic
422 species (SO_4^{2-} and metals) due to incomplete combustion and lack of pollution control

423 devices (Garcia et al., 1992; Li et al., 2016; Watson et al., 2001a, b). Garcia et al. (1992)
424 studied emissions of volatile organic compounds from coal burning and vehicle engines.
425 In Ulaanbaatar, the use of wood and coal for cooking and heating, and emissions
426 from old vehicles are reported as potential sources of OC (Batmunkh et al., 2013;
427 Zhamsueva et al., 2018). The three thermal power plants in Ulaanbaatar are point
428 sources for emissions of carbonaceous aerosol (Batmunkh et al., 2013), burning ~5
429 million tons of coal per year (Batmunkh et al., 2013). High concentrations of anions
430 (SO_4^{2-} and NO_3^-) and cations (NH_4^+ and Na^+) are reported in China (Zhou et al., 2003),
431 the USA (Caiazzo et al., 2013), Brazil (Flues et al., 2002), India (Guttikunda and
432 Jawahar, 2014), Korea (Park and Kim, 2004; Park et al., 2015), and Spain (Alastuey et
433 al., 1999) near coal-fired thermal power plants. Emissions of volatile organic
434 compounds from vegetation have also been observed in previous studies (Fehsenfeld et
435 al., 1992; Shao et al., 2001; Acton et al., 2016). The correlations of $OC_{non\text{-}BB}$ with ions
436 and EC are thus likely due to volatile organic compounds emitted from coal-burning
437 and vehicles, and vegetative emissions.
438
439 **4. Conclusions**
440 BB was identified as a major source of the quantified aerosol components in $PM_{2.5}$
441 in Ulaanbaatar, Mongolia, during the winter and spring of 2017, based on PCA. OC was
442 the major component of the quantified aerosol components during the entire sampling
443 period, winter and spring. For determination of OC_{BB}, the fuel type must be identified
444 and levoglucosan/mannosan and levoglucosan/K^+ ratios obtained from previous studies
445 and our on-site measurements were used for this purpose.
446 Softwood burning was identified as a major source of OC_{BB}. However,

OC/levoglucosan ratios from softwood burning are highly variable, and an optimum ratio was derived by regression analysis between daily concentrations of $OC_{non\text{-}BB}$ and levoglucosan, yielding values of 27.6 and 18.0 for winter and spring, respectively. The application of these ratios indicates that 68% and 63% of the OC originated from BB during winter and spring, respectively, which is about double that estimated using average values of previous studies. The atmospheric concentration of OC_{BB} was higher in winter than in spring mainly due to additional BB for heating and cooking. BB aerosols in Ulaanbaatar originate mainly from local softwood burning. The approach developed here may be applied elsewhere for screening region-specific OC/levoglucosan ratios for estimating atmospheric appropriate concentrations of OC_{BB}, aiding the establishment of BB control measures.

Author contribution

Jinsang Jung and Tsatsral Batmunkh designed the study and carried out the field work. Jinsang Jung performed chemical analyses and quality-control measures. Jayant Nirmalkar wrote the manuscript under the guidance of Jinsang Jung. All authors commented on and discussed the manuscript.

Competing interests

The authors declare that they have no conflict of interests.

Acknowledgments

This work was funded by a grant (19011057) from the Korea Research Institute of

Standards and Science (KRISS) under the Basic R&D Project of Quantification of local and long-range transported pollutants during a severe haze episode over the Korean Peninsula. The authors gratefully acknowledge the NOAA Air Resources Laboratory for the provision of the HYSPLIT transport and dispersion model and access to the READY website (http://www.arl.noaa.gov/ready.html) and the Fire Information for Resource Management System (FIRMS) of the National Aeronautics and Space Administration (NASA), United States (https://firms.modaps.eosdis.nasa.gov/alerts/) used in this study.

Data availability

The data used in this study are available from the corresponding author upon request (jsjung@kriss.re.kr).

References

Achad, M., Caumo, S., de Castro Vasconcellos, P., Bajano, H., Gómez, D., and Smichowski, P.: Chemical markers of biomass burning: Determination of levoglucosan, and potassium in size-classified atmospheric aerosols collected in Buenos Aires, Argentina by different analytical techniques, Microchem. J., 139, 181−187, https://doi.org/10.1016/j.microc.2018.02.016, 2018.

Acton, W. J. F., Schallhart, S., Langford, B., Valach, A., Rantala, P., Fares, S., and Carriero, G.: Canopy−scale flux measurements and bottom-up emission estimates of volatile organic compounds from a mixed oak and hornbeam forest in northern Italy, Atmos. Chem. Phys., 16, 7149−7170, https://doi.org/10.5194/acp-16-7149-2016, 2016.

Alastuey, A., Querol, X., Chaves, A., Ruiz, C. R., Carratala, A., and Lopez−Soler, A.: Bulk deposition in a rural area located around a large coal-fired power station, northeast Spain, Environ. Pollut., 106(3), 359−367, https://doi.org/10.1016/S0269-7491(99)00103-7, 1999.

Allan, J. D., Morgan, W. T., Darbyshire, E., Flynn, M. J., Williams, P. I., Oram, D. E., Artaxo, P., Brito, J., Lee, J. D., and Coe, H.: Airborne observations of IEPOX-derived isoprene SOA in the Amazon during SAMBBA, Atmos. Chem. Phys., 14, 11393–11407, https://doi.org/10.5194/acp-14-11393-2014, 2014.

Ashbaugh, L.L., Malm, W.C., and Sadeh, W.Z.: A residence time probability analysis of sulfur concentrations at Grand Canyon National Park, Atmos. Environ., 19(8), 1263−1270, https://doi.org/10.1016/0004-6981(85)90256-2, 1985.

Bari, M. A., Baumbach, G., Kuch, B., and Scheffknecht, G.: Wood smoke as a source of particle-phase organic compounds in residential areas, Atmos. Environ., 43, 4722−4732, https://doi.org/10.1016/j.atmosenv.2008.09.006, 2009.

Batmunkh, T., Kim, Y. J., Jung, J. S., Park, K., and Tumendemberel, B.: Chemical characteristics of fine particulate matters measured during severe winter haze events in Ulaanbaatar, Mongolia, J. Air & Waste Manag. Assoc., 63, 659−670, https://doi.org/10.1080/10962247.2013.776997, 2013.

Caiazzo, F., Ashok, A., Waitz, I. A., Yim, S. H., and Barrett, S. R.: Air pollution and early deaths in the United States. Part I: Quantifying the impact of major sectors in 2005, Atmos. Environ., 79, 198−208,

https://doi.org/10.1016/j.atmosenv.2013.05.081, 2013.

Cao, J. J., Wu, F., Chow, J. C., Lee, S. C., Li, Y., Chen, S. W., An, Z. S., Fung, K. K., Watson, J. G., Zhu, C. S., and Liu, S. X.: Characterization and source apportionment of atmospheric organic and elemental carbon during fall and winter of 2003 in Xi'an, China, Atmos. Chem. Phys., 5, 3127−3137, https://doi.org/10.5194/acp-5-3127-2005, 2005.

Chantara, S., Thepnuan, D., Wiriya, W., Prawan, S., and Tsai, Y. I.: Emissions of pollutant gases, fine particulate matters and their significant tracers from biomass burning in an open-system combustion chamber, Chemosphere, 224, 407−416, 2019.

Chen, H., Yin, S., Li, X., Wang, J., and Zhang, R.: Analyses of biomass burning contribution to aerosol in Zhengzhou during wheat harvest season in 2015, Atmos. Res., 207, 62−73, https://doi.org/10.1016/j.atmosres.2018.02.025, 2018.

Cheng, Y., Engling, G., He, K.-B., Duan, F.-K., Ma, Y.-L., Du, Z.-Y., Liu, J.-M., Zheng, M., and Weber, R. J.: Biomass burning contribution to Beijing aerosol, Atmos. Chem. Phys., 13, 7765−7781, https://doi.org/10.5194/acp-13-7765-2013, 2013.

Chung, S. and Chon, H. T.: Assessment of the level of mercury contamination from some anthropogenic sources in Ulaanbaatar, Mongolia, J. Geochem. Explor., 147, 237−244, https://doi.org/10.1016/j.gexplo.2014.07.016, 2014.

Claeys, M., Kourtchev, I., Pashynska, V., Vas, G., Vermeylen, R., Wang, W., Cafmeyer, J., Chi, X., Artaxo, P., Andreae, M. O., and Maenhaut, W.: Polar organic marker compounds in atmospheric aerosols during the LBA-SMOCC 2002 biomass burning experiment in Rondônia, Brazil: sources and source processes, time series, diel variations and size distributions, Atmos. Chem. Phys., 10, 9319−9331, https://doi.org/10.5194/acp-10-9319-2010, 2010.

Deshmukh, D. K., Deb, M. K., Tsai, Y. I., and Mkoma, S. L.: Water soluble ions in PM2.5 and PM1 aerosols in Durg city, Chhattisgarh, India, Aerosol Air Qual. Res, 11, 696-708, 10.4209/aaqr.2011.03.0023, 2011.

Deshmukh, D. K., Haque, M. M., Kim, Y., and Kawamura, K.: Organic tracers of fine aerosol particles in central Alaska: summertime composition and sources, Atmos. Chem. Phys., 19, 14009–14029, https://doi.org/10.5194/acp-19-14009-2019, 2019.

Davy, P. K., Gunchin, G., Markwitz, A., Trompetter, W. J., Barry, B. J., Shagjjamba, D.,

and Lodoysamba, S.: Air particulate matter pollution in Ulaanbaatar, Mongolia: determination of composition, source contributions and source locations, Atmos. Poll. Res., 2, 126-137, https://doi.org/10.5094/APR.2011.017, 2011.

Duan, F., Liu, X., Yu, T., and Cachier, H.: Identification and estimate of biomass burning contribution to the urban aerosol organic carbon concentrations in Beijing, Atmos. Environ. 38, 1275−1282, https://doi.org/10.1016/j.atmosenv.2003.11.037, 2004.

Engling, G., Carrico, C. M., Kreidenweis, S. M., Collett Jr., J. L., Day, D. E., Malm, W. C., Lincoln, L., Hao, W. M., Iinuma, Y., and Herrmann, H.: Determination of levoglucosan in biomass combustion aerosol by high-performance anion-exchange chromatography with pulsed amperometric detection, Atmos. Environ., 40, 299−311, https://doi.org/10.1016/j.atmosenv.2005.12.069, 2006.

Engling, G., Lee, J. J., Tsai, Y. W., Lung, S. C. C., Chou, C. C. K., and Chan, C. Y.: Size resolved anhydrosugar composition in smoke aerosol from controlled field burning of rice straw, Aerosol Sci. Technol., 43, 662−672, https://doi.org/10.1080/02786820902825l1, 2009.

Fang, G. C., Chang, C. N., Chu, C. C., Wu, Y. S., Fu, P. P. C., Yang, I. L., and Chen, M. H.: Characterization of particulate, metallic elements of TSP, $PM_{2.5}$ and $PM_{2.5-10}$ aerosols at a farm sampling site in Taiwan, Taichung, Sci. Tot. Environ., 308, 157−166, https://doi.org/10.1016/S0048-9697(02)00648-4, 2003.

Fehsenfeld, F., Calvert, J., Fall, R., Goldan, P., Guenther, A. B., Hewitt, C. N., Lamb, B., Liu, S., Trainer, M., Westberg, H., and Zimmerman, P.: Emissions of volatile organic compounds from vegetation and the implications for atmospheric chemistry, Global Biogeochem. Cy., 6, 389−430, https://doi.org/10.1029/92GB02125, 1992.

Feng, Y., Chen, Y., Guo, H., Zhi, G., Xiong, S., Li, J., Sheng, G., and Fu, J.: Characteristics of organic and elemental carbon in $PM_{2.5}$ samples in Shanghai, China, Atmos. Res., 92, 434−442, https://doi.org/10.1016/j.atmosres.2009.01.003, 2009.

Fine, P. M., Cass, G. R., and Simoneit, B. R. T.: Chemical characterization of fine particle emissions from fireplace combustion of woods grown in the northeastern United States, Environ. Sci. Technol., 35, 2665−2675,

https://doi.org/10.1021/es001466k, 2001.

Fine, P. M., Cass, G. R., and Simoneit, B. R. T.: Chemical characterization of fine particle emissions from the fireplace combustion of woods grown in the southern United States, Environ. Sci. Technol., 36, 1442−1451, https://doi.org/10.1021/es0108988, 2002.

Fine, P. M., Cass, G. R., and Simoneit, B. R. T.: Chemical characterization of fine particle emissions from the fireplace combustion of wood types grown in the midwestern and western United States, Environ. Engin. Sci., 21, 387−409, https://doi.org/10.1089/109287504323067021, 2004a.

Fine, P. M., Cass, G. R., and Simoneit, B. R. T.: Chemical characterization of fine particle emissions from the wood stove combustion of prevalent United States tree species, Environ. Engin. Sci., 21, 705−721, https://doi.org/10.1089/ees.2004, 21.705, 2004b.

Flues, M., Hama, P., Lemes, M. J. L., Dantas, E. S. K., and Fornaro, A.: Evaluation of the rainwater acidity of a rural region due to a coal-fired power plant in Brazil, Atmos. Environ., 36, 2397−2404, https://doi.org/10.1016/S1352-2310(01)00563-5, 2002.

Fu, P. Q., Kawamura, K., Chen, J., Li, J., Sun, Y. L., Liu, Y., Tachibana, E., Aggarwal, S. G., Okuzawa, K., Tanimoto, H., and Kanaya, Y.: Diurnal variations of organic molecular tracers and stable carbon isotopic composition in atmospheric aerosols over Mt. Tai in the North China Plain: an influence of biomass burning, Atmos. Chem. Phys., 12, 8359−8375, doi:10.5194/acp-12-8359-2012, 2012.

Gao, S., Hegg D. A., Hobbs P. V., Kirchstetter T. W., Magi B. I., and Sadilek M.: Water-soluble organic components in aerosols associated with savanna fires in southern Africa: Identification, evolution, and distribution, J. Geophys. Res., 108(D13), 8491, doi:10.1029/2002JD002324, 2003.

Garcia, J., Beyne-Masclet, S., Mouvier, G., and Masclet, P.: Emissions of volatile organic compounds by coal-fired power stations. Atmos. Environ., Part A, 26, 1589−1597, https://doi.org/10.1016/0960-1686(92)90059-T, 1992.

Gonçalves, C., Alves, C., Evtyugina, M., Mirante, F., Pio, C., Caseiro, A., Schmidl, C., Bauer, H., and Carvalho, F.: Characterisation of PM_{10} emissions from wood stove combustion of common woods grown in Portugal, Atmos. Environ., 44,

4474−4480, https://doi.org/10.1016/j.atmosenv.2010.07.026, 2010.

Gu, J., Bai, Z., Li, W., Wu, L., Liu, A., Dong, H., and Xie, Y.: Chemical composition of $PM_{2.5}$ during winter in Tianjin, China, Particuology, 9, 215−221, https://doi.org/10.1016/j.partic.2011.03.001, 2011.

Guttikunda, S.: Urban air pollution analysis for Ulaanbaatar, Mongolia, SIM Working Paper No. 2008-005, http://dx.doi.org/10.2139/ssrn.1288328, 2008.

Guttikunda, S. K. and Jawahar, P.: Atmospheric emissions and pollution from the coal−fired thermal power plants in India, Atmos. Environ., 92, 449−460, https://doi.org/10.1016/j.atmosenv.2014.04.057, 2014.

Harrison, R. M., Beddows, D. C. S., Hu, L., and Yin, J.: Comparison of methods for evaluation of wood smoke and estimation of UK ambient concentrations, Atmos. Chem. Phys., 12, 8271−8283, doi:10.5194/acp−12−8271−2012, 2012.

Hays, M. D., Geron, C. D., Linna, K. J., Smith, N. D., and Schauer, J. J.: Speciation of gasphase and fine particle emissions from burning of foliar fuels, Environ. Sci. Technol., 36, 2281−2295, https://doi.org/10.1021/es0111683, 2002.

Haque, M., Kawamura, K., Deshmukh, D. K., Fang, C., Song, W., Mengying, B., and Zhang, Y. L.: Characterization of organic aerosols from a Chinese megacity during winter: predominance of fossil fuel combustion. Atmos. Chem. Phys., 19, 5147-5164, https://doi.org/10.5194/acp-19-5147-2019, 2019.

Huang, X., Liu, Z., Zhang, J., Wen, T., Ji, D., and Wang, Y.: Seasonal variation and secondary formation of size-segregated aerosol water-soluble inorganic ions during pollution episodes in Beijing, Atmos. Res., 168, 70−79, https://doi.org/10.1016/j.atmosres.2015.08.021, 2016.

Iinuma, Y., Brüggemann, E., Gnauk, T., Müller, K., Andreae, M. O., Helas, G., Parmar, R., and Herrmann, H.: Source characterization of biomass burning particles: the combustion of selected European conifers, African hardwood, savanna grass, and German and Indonesian peat, J. Geophys. Res., 112, D08209. http://dx.doi.org/10.1029/2006JD007120, 2007.

Ji, D., Zhang, J., He, J., Wang, X., Pang, B., Liu, Z., Wang, L., and Wang, Y.: Characteristics of atmospheric organic and elemental carbon aerosols in urban Beijing, China, Atmos. Environ., 125, 293−306, https://doi.org/10.1016/j.atmosenv.2015.11.020, 2016.

Jimenez, J. L., Canagaratna, M. R., Donahue, N. M., Prevot, A. S. H., Zhang, Q., Kroll, J. H., DeCarlo, P. F., Allan, J. D., Coe, H., Ng, N. L., and Aiken, A. C.: Evolution of organic aerosols in the atmosphere, Science, 326, 1525−1529, doi:10.1126/science.1180353, 2009.

Jung, J., Lee, H., Kim ,Y. J., Liu, X., Zhang, Y., Hu, M., and Sugimoto, N.: Optical properties of atmospheric aerosols obtained by in situ and remote measurements during 2006 Campaign of Air Quality Research in Beijing (CAREBeijing-2006), J. Geophys. Res., 114, D00G02, doi:10.1029/2008JD010337, 2009.

Jung, J., Tsatsral, B., Kim, Y. J., and Kawamura, K.: Organic and inorganic aerosol compositions in Ulaanbaatar, Mongolia, during the cold winter of 2007 to 2008: dicarboxylic acids, ketocarboxylic acids, and α-dicarbonyls, J. Geophys. Res.: Atmos., 115, D22203, https://doi.org/10.1029/2010JD014339, 2010.

Jung, J., Lee, S., Kim, H., Kim, D., Lee, H., and Oh, S.: Quantitative determination of the biomass-burning contribution to atmospheric carbonaceous aerosols in Daejeon, Korea, during the rice-harvest period, Atmos. Environ., 89, 642−650, https://doi.org/10.1016/j.atmosenv.2014.03.010, 2014.

Khan, M. F., Shirasuna, Y., Hirano, K., and Masunaga, S.: Characterization of $PM_{2.5}$, $PM_{2.5–10}$ and $PM_{>10}$ in ambient air, Yokohama, Japan, Atmos. Res., 96, 159-172, https://doi.org/10.1016/j.atmosres.2009.12.009, 2010.

Klejnowski, K., Janoszka, K., and Czaplicka, M.: Characterization and seasonal variations of organic and elemental carbon and levoglucosan in PM10 in Krynica Zdroj, Poland, Atmosphere, 8, 190, doi:10.3390/atmos8100190, 2017.

Lai, C., Liu, Y., Ma, J., Ma, Q., and He, H.: Degradation kinetics of levoglucosan initiated by hydroxyl radical under different environmental conditions, Atmos. Environ., 91, 32−39, https://doi.org/10.1016/j.atmosenv.2014.03.054, 2014.

Lee, T., Sullivan, A. P., Mack, L., Jimenez, J. L., Kreidenweis, S. M., Onasch, T. B., Worsnop, D. R., Malm, W., Wold, C. E., Hao, W. M., and Collett Jr, J. L.: Chemical smoke marker emissions during flaming and smoldering phases of laboratory open burning of wildland fuels, Aerosol Sci. Technol., 44, i-v, https://doi.org/10.1080/02786826.2010.499884, 2010.

Li, Q., Jiang, J., Zhang, Q., Zhou, W., Cai, S., Duan, L., Ge, S., and Hao, J.: Influences of coal size, volatile matter content, and additive on primary particulate matter

675 emissions from household stove combustion. Fuel, 182, 780-787,
676 https://doi.org/10.1016/j.fuel.2016.06.059, 2016.
677 Liang, L., Engling, G., Du, Z., Cheng, Y., Duan, F., Liu, X., and He, K.: Seasonal
678 variations and source estimation of saccharides in atmospheric particulate matter
679 in Beijing, China, Chemosphere, 150, 365−377,
680 https://doi.org/10.1016/j.chemosphere.2016.02.002, 2016.
681 Lin, Y.-C., Hsu, S.-C., Lin, C.-Y., Lin, S.-H., Huang, Y.-T., Chang, Y., and Zhang, Y.-L.:
682 Enhancements of airborne particulate arsenic over the subtropical free troposphere:
683 impact of southern Asian biomass burning, Atmos. Chem. Phys., 18, 13865-13879,
684 https://doi.org/10.5194/acp-18-13865−2018, 2018.
685 Louie, P. K., Watson, J. G., Chow, J. C., Chen, A., Sin, D. W., and Lau, A. K.: Seasonal
686 characteristics and regional transport of $PM_{2.5}$ in Hong Kong, Atmos. Environ., 39,
687 1695−1710, https://doi.org/10.1016/j.atmosenv.2004.11.017, 2005.
688 Maenhaut, W., Nava, S., Lucarelli, F., Wang, W., Chi, X., and Kulmala, M.: Chemical
689 composition, impact from biomass burning, and mass closure for $PM_{2.5}$ and PM_{10}
690 aerosols at Hyytiälä, Finland, in summer 2007, X-Ray Spectrom., 40, 168−171,
691 https://doi.org/10.1002/xrs.1302, 2011.
692 Nirmalkar, J., Deshmukh, D. K., Deb, M. K., Tsai, Y. I., and Sopajaree, K.: Mass
693 loading and episodic variation of molecular markers in $PM_{2.5}$ aerosols over a rural
694 area in eastern central India, Atmos. Environ., 117, 41–50,
695 https://doi.org/10.1016/j.atmosenv.2015.07.003, 2015.
696 Nirmalkar, J., Deshmukh, D. K., Deb, M. K., Tsai, Y. I., and Pervez, S.: Characteristics
697 of aerosol during major biomass burning events over eastern central India in
698 winter: A tracer-based approach, Atmos. Pollut. Res., 10, 817−826,
699 https://doi.org/10.1016/j.apr.2018.12.010, 2019.
700 Oanh, N. T. K., Ly, B. T., Tipayarom, D., Manandhar, B. R., Prapat, P., Simpson, C.D.,
701 and Liu, L.J.S.: Characterization of particulate matter emission from open burning
702 of rice straw, Atmos. Environ., 45, 493−502,
703 https://doi.org/10.1016/j.atmosenv.2010.09.023, 2011.
704 Obrist, D., Moosmüller, H., Schürmann, R., Chen, L. W. A., and Kreidenweis, S. M.:
705 Particulate-phase and gaseous elemental mercury emissions during biomass
706 combustion: controlling factors and correlation with particulate matter emissions.

Environ. Sci. Technol., 42, 721-727, https://doi.org/10.1021/es071279n, 2007.

Panda, S., Sharma, S. K., Mahapatra, P. S., Panda, U., Rath, S., Mahapatra, M., Mandal, T. K., and Das, T.: Organic and elemental carbon variation in $PM_{2.5}$ over megacity Delhi and Bhubaneswar, a semi-urban coastal site in India, Nat. Hazards, 80, 1709−1728, https://doi.org/10.1007/s11069-015-2049-3, 2016.

Park, S. S. and Kim, Y. J.: $PM_{2.5}$ particles and size-segregated ionic species measured during fall season in three urban sites in Korea, Atmos. Environ., 38, 1459–1471, https://doi.org/10.1016/j.atmosenv.2003.12.004, 2004.

Park, S. M., Seo, B. K., Lee, G., Kahng, S. H., and Jang, Y.: Chemical composition of water-soluble inorganic species in precipitation at Shihwa Basin, Korea, Atmosphere, 6, 732−750, https://doi.org/10.3390/atmos6060732, 2015.

Pei, B., Wang, X., Zhang, Y., Hu, M., Sun, Y., Deng, J., Dong, L., Fu, Q., and Yan N.: Emissions and source profiles of PM2.5 for coal-fired boilers in the Shanghai megacity, China, Atmos. Pollut. Res. 7, 577-584, https://doi.org/10.1016/j.apr.2016.01.005, 2016.

Pio, C. A., Legrand, M., Alves, C. A., Oliveira, T., Afonso, J., Caseiro, A., Puxbaum, H., Sanchez−Ochoa, A., and Gelencser, A.: Chemical composition of atmospheric aerosols during the 2003 summer intense forest fire period, Atmos. Environ., 42, 7530−7543, https://doi.org/10.1016/j.atmosenv.2008.05.032, 2008.

Puxbaum, H., Caseiro, A., Sánchez-Ochoa, A., Kasper-Giebl, A., Claeys, M., Gelencser, A., Legrand, M., Preunkert, S., and Pio, C.: Levoglucosan levels at background sites in Europe for assessing the impact of biomass combustion on the European aerosol background, J. Geophys. Res.: Atmos., 112, D23S05, https://doi.org/10.1029/2006JD008114, 2007.

Reche, C., Viana, M., Amato, F., Alastuey, A., Moreno, T., Hillamo, R., Teinila, K., Saarnio, K., Seco, R., Penuelas, J., and Mohr, C.: Biomass burning contributions to urban aerosols in a coastal Mediterranean City, Sci. Tot. Environ., 427, 175−190, https://doi.org/10.1016/j.scitotenv.2012.04.012, 2012.

Schauer, J.J., Kleeman, M.J., Cass, G.R., and Simoneit, B. R. T.: Measurement of emissions from air pollution sources. 3. C1-C29 organic compounds from fireplace combustion of wood, Environ. Sci. Technol., 35, 1716−1728, https://doi.org/10.1021/es001331e, 2001.

739 Schkolnik, G., Falkovich, A. H., Rudich, Y., Maenhaut, W., and Artaxo, P.: New
740 analytical method for the determination of levoglucosan, polyhydroxy compounds,
741 and 2-methylerythritol and its application to smoke and rainwater samples,
742 Environ. Sci. Technol. 39, 2744−2752, https://doi.org/10.1021/es048363c, 2005.
743 Schmidl, C., Marr, I. L., Caseiro, A., Kotianová, P., Berner, A., Bauer, H., Kasper-Giebl,
744 A., and Puxbaum, H.: Chemical characterisation of fine particle emissions from
745 wood stove combustion of common woods growing in mid-European Alpine
746 regions, Atmos. Environ., 42, 126−141,
747 https://doi.org/10.1016/j.atmosenv.2007.09.028, 2008.
748 Shao, M., Czapiewski, K. V., Heiden, A. C., Kobel, K., Komenda, M., Koppmann, R.,
749 and Wildt, J.: Volatile organic compound emissions from Scots pine: mechanisms
750 and description by algorithms, J. Geophys. Res.: Atmos., 106(D17), 20483−20491,
751 10.1029/2000JD000248, 2001.
752 Sharma, A., Pareek, V., and Zhang, D.: Biomass pyrolysis—A review of modelling,
753 process parameters and catalytic studies. J. Renew. Sustain. Energy, 50,
754 1081−1096, https://doi.org/10.1016/j.rser.2015.04.193, 2015.
755 Sheesley, R. J., Schauer, J. J., Chowdhury, Z., Cass, G. R., and Simoneit, B. R. T.:
756 Characterization of organic aerosols emitted from the combustion of biomass
757 indigenous to South Asia, J. Geophys. Res., 108, 4285, http://
758 dx.doi.org/10.1029/2002JD002981, 2003.
759 Simoneit, B. R., Schauer, J. J., Nolte, C. G., Oros, D. R., Elias, V. O., Fraser, M. P.,
760 Rogge, W. F., and Cass, G. R., 1999. Levoglucosan, a tracer for cellulose in
761 biomass burning and atmospheric particles, Atmos. Environ., 33, 173−182,
762 https://doi.org/10.1016/S1352-2310(98)00145-9, 1999.
763 Sullivan, A. P., Holden, A. S., Patterson, L. A., McMeeking, G. R., Kreidenweis, S. M.,
764 Malm, W. C., Hao, W. M., Wold, C. E., and Collett Jr., J. L.: A method for smoke
765 marker measurements and its potential application for determining the
766 contribution of biomass burning from wildfires and prescribed fires to ambient
767 $PM_{2.5}$ organic carbon, J Geophys. Res., 113, D22302, http://
768 dx.doi.org/10.1029/2008JD010216, 2008.
769 Sullivan, A. P., Guo, H., Schroder, J. C., Campuzano-Jost, P., Jimenez, J. L., Campos, T.,
770 Shah, V., Jaegle, L., Lee, B. H., Lopez-Hilfiker, F. D., and Thornton, J. A.:

Biomass burning markers and residential burning in the winter aircraft campaign. J. Geophys. Res.: Atmos., 124, 1846−1861, https://doi.org/10.1029/2017JD028153, 2019.

Sun, J., Shen, Z., Zhang, Y., Zhang, Q., Wang, F., Wang, T., Chang, X., Lei, Y., Xu, H., Cao, J., and Zhang, N.: Effects of biomass briquetting and carbonization on PM2.5 emission from residential burning in Guanzhong Plain, China, Fuel, 244, 379−387, https://doi.org/10.1016/j.fuel.2019.02.031, 2019.

Tao, J., Zhang, L., Ho, K., Zhang, R., Lin, Z., Zhang, Z., Lin, M., Cao, J., Liu, S., and Wang, G.: Impact of $PM_{2.5}$ chemical compositions on aerosol light scattering in Guangzhou—the largest megacity in South China, Atmos. Res., 135, 48−58, https://doi.org/10.1016/j.atmosres.2013.08.015, 2014.

Thepnuan, D., Chantara, S., Lee, C. T., Lin, N. H., and Tsai, Y. I.: Molecular markers for biomass burning associated with the characterization of $PM_{2.5}$ and component sources during dry season haze episodes in Upper South East Asia, Sci. Tot. Environ., 658, 708−722, https://doi.org/10.1016/j.scitotenv.2018.12.201, 2019.

Verma, V., Fang, T., Guo, H., King, L., Bates, J. T., Peltier, R. E., Edgerton, E., Russell, A. G., and Weber, R. J.: Reactive oxygen species associated with water-soluble PM2.5 in the southeastern United States: spatiotemporal trends and source apportionment, Atmos. Chem. Phys., 14, 12915-12930, https://doi.org/10.5194/acp-14-12915-2014, 2014.

Wang, T., Tian, M., Ding, N., Yan, X., Chen, S. J., Mo, Y. Z., Yang, W. Q., Bi, X. H., Wang, X. M., and Mai, B. X.: Semivolatile organic compounds (SOCs) in fine particulate matter ($PM_{2.5}$) during clear, fog, and haze episodes in winter in Beijing, China, Environ. Sci. Tech., 52, 5199−5207, https://doi.org/10.1021/acs.est.7b06650, 2018.

Watson, J. G., Chow, J. C., and Fujita, E. M.: Review of volatile organic compound source apportionment by chemical mass balance, Atmos. Environ., 35, 1567−1584, https://doi.org/10.1016/S1352-2310(00)00461-1, 2001a.

Watson, J. G., Chow, J. C., and Houck, J. E.: $PM_{2.5}$ chemical source profiles for vehicle exhaust, vegetative burning, geological material, and coal burning in Northwestern Colorado during 1995, Chemosphere, 43, 1141−1151, https://doi.org/10.1016/S0045-6535(00)00171-5, 2001b.

Zhamsueva, G. S., Zayakhanov, A. S., Starikov, A. V., Balzhanov, T. S., Tsydypov, V. V., Dementyeva, A. L., and Khodzher, T. V.: Investigation of chemical composition of atmospheric aerosol in Ulaanbaatar during 2005–2014. Geography and Natural 39, 270−276, 10.1134/S1875372818030113, 2018

Zhang, F., Wang, Z. W., Cheng, H. R., Lv, X. P., Gong, W., Wang, X. M., and Zhang, G.: Seasonal variations and chemical characteristics of $PM_{2.5}$ in Wuhan, central China, Sci. Tot. Environ., 518, 97−105, https://doi.org/10.1016/j.scitotenv.2015.02.054, 2015.

Zhang, Y. X., Min, S., Zhang, Y. H., Zeng, L. M., He, L. Y., Bin, Z. H. U., Wei, Y. J., and Zhu, X. L.: Source profiles of particulate organic matters emitted from cereal straw burnings. J. Environ. Sci., 19, 167−175, https://doi.org/10.1016/S1001-0742(07)60027-8, 2007.

Zhou, Y., Levy, J. I., Hammitt, J. K., and Evans, J. S.: Estimating population exposure to power plant emissions using CALPUFF: a case study in Beijing, China, Atmos. Environ., 37, 815−826, https://doi.org/10.1016/S1352-2310(02)00937-8, 2003.

Zhu, C., Kawamura, K., and Kunwar, B.: Effect of biomass burning over the western North Pacific Rim: wintertime maxima of anhydrosugars in ambient aerosols from Okinawa, Atmos. Chem. Phys., 15, 1959−1973, https://doi.org/10.5194/acp-15-1959-2015, 2015.

Table 1. Concentrations (μg m^{-3}) of organic carbon, elemental carbon, levoglucosan, mannosan, galactosan, and water-soluble ions in $PM_{2.5}$ samples collected from Ulaanbaatar, Mongolia, during the winter (n = 17) and spring (n = 17) of 2017.

	OC	EC	Levoglucosan	Mannosan	Galactosan	Cl^-	SO_4^{2-}	NO_3^-	Na^+	NH_4^+	K^+	Mg^{2+}	Ca^{2+}	Temperature (°C)	Wind Speed (m sec^{-1})	RH (%)
Winter																
Mean	49.06	1.71	1.20	0.33	0.24	1.69	9.74	4.17	0.64	6.18	0.13	0.05	0.60	-20.8	1.36	66.1
SD	17.32	0.58	0.43	0.13	0.09	0.76	3.37	1.69	0.44	2.42	0.04	0.02	0.24	4.74	0.73	4.56
Min	24.62	0.79	0.58	0.15	0.10	0.26	2.17	0.76	0.10	3.16	0.08	0.02	0.22	-27.8	0.41	58.5
Max	79.07	3.34	2.12	0.61	0.43	2.89	16.06	7.51	1.34	11.59	0.18	0.08	1.04	-10.5	3.55	72.7
Spring																
Mean	8.50	1.11	0.31	0.08	0.04	0.30	1.90	0.70	0.13	0.74	0.08	0.04	0.93	6.11	2.60	35.1
SD	3.55	0.42	0.18	0.04	0.02	0.11	0.50	0.32	0.04	0.28	0.05	0.02	0.36	6.16	0.79	13.9
Min	2.80	0.60	0.03	0.01	0.00	0.11	1.04	0.10	0.07	0.33	0.02	0.02	0.48	-1.52	1.64	17.8
Max	16.63	2.03	0.73	0.15	0.08	0.51	3.02	1.40	0.21	1.47	0.22	0.08	1.61	15.9	4.56	65.2

Table 2. Source identification of chemical species using principal component (PC) analysis and varimax rotation at Ulaanbaatar, Mongolia, during winter of 2017.

Winter	Component			
Chemical species	PC1 (Biomass Burning)	PC2 (Dust)	PC3 (Secondary formation)	PC4 (Fossil fuel combustion)
Levoglucosan	**0.96**	−0.06	0.24	0.06
Mannosan	**0.95**	−0.08	0.27	0.06
Galactosan	**0.95**	−0.07	0.28	0.04
Cl^-	0.19	**0.94**	−0.05	−0.07
SO_4^{2-}	0.43	0.01	**0.88**	0.09
NO_3^-	0.28	0.20	**0.87**	0.20
Na^+	−0.27	**0.87**	−0.33	−0.17
NH_4^+	0.48	−0.12	**0.86**	0.07
K^+	**0.70**	0.11	0.61	0.25
Mg_2^+	−0.15	**0.90**	0.25	0.26
Ca_2^+	−0.12	**0.92**	0.19	0.24
OC	**0.82**	−0.17	0.47	0.07
EC	0.14	0.14	0.19	**0.95**
Eigenvalues	4.54	3.44	3.30	1.20
% of Variance	34.95	26.49	25.37	9.21
Cumulative %	34.95	61.44	86.81	96.02

839 Table 3. Source identification of chemical species using PCA and varimax rotation at Ulaanbaatar, Mongolia, during spring of 2017.

Spring	Component		
Chemical species	PC1 (Biomass Burning)	PC2 (Dust and Fossil fuel combustion)	PC3 (Secondary formation)
Levoglucosan	**0.88**	0.13	0.39
Mannosan	**0.94**	0.00	0.30
Galactosan	**0.95**	−0.11	0.20
Cl^-	**0.81**	0.32	−0.03
SO_4^{2-}	0.18	0.12	**0.93**
NO_3^-	0.59	0.54	0.52
Na^+	0.08	**0.91**	−0.09
NH_4^+	0.44	0.05	**0.88**
K^+	0.41	0.67	0.55
Mg^{2+}	0.05	**0.90**	0.35
Ca^{2+}	0.10	**0.97**	0.15
OC	**0.77**	0.41	0.46
EC	0.10	**0.94**	0.01
Eigenvalues	4.59	4.53	2.87
% of Variance	35.30	34.84	22.04
Cumulative %	35.30	70.14	92.18

840

Table 4. Correlation coefficients (r) from Spearman correlation analysis for $OC_{non\text{-}BB}$ and water-soluble ions during winter and spring of 2017 at Ulaanbaatar, Mongolia.

		Cl^-	SO_4^{2-}	NO_3^-	Na^+	NH_4^+	K^+	Mg^{2+}	Ca^{2+}	EC
$OC_{non\text{-}BB}$	Winter	−0.26	0.71**	0.44	−0.58*	0.72**	0.64**	−0.16	−0.16	0.15
	Spring	0.29	0.37	0.59*	0.74**	0.23	0.65**	0.78**	0.77**	0.74**

*Correlation is significant at the .05 level (2-tailed); **Correlation is significant at the .01 level (2-tailed).

Figure captions

Fig. 1 Sampling site in Ulaanbataar, Mongolia (https://www.google.com/earth/versions/#earth-pro, © Google Earth).

Fig. 2 Daily variations in atmospheric concentrations (μg m^{-3}) of chemical species in Ulaanbaatar during winter (a) and spring (b) of 2017.

Fig. 3 Daily atmospheric concentrations of OC (μg C m^{-3}) as a function of wind speed (m s^{-1}) and temperature (°C) during winter (a) and spring (b) of 2017.

Fig. 4 Relationship between $PM_{2.5}$ concentrations of $Ca^{2+}$and EC (μg m^{-3}) during spring of 2017.

Fig. 5 Conditional Probability Function (CPF) of levoglucosan (levo), OC, K^+, EC, Ca^{2+} during winter (a) and spring (b) of 2017.

Fig. 6 (a) Five-day backward air-mass trajectories (https://ready.arl.noaa.gov/HYSPLIT.php) and (b) FIRMS fire counts (https://firms.modaps.eosdis.nasa.gov/alerts/) around Ulaanbaatar during spring of 2017.

Fig. 7 Correlations of $PM_{2.5}$ concentrations (μg m^{-3}) of mannosan and galactosan with levoglucosan during winter (a) and spring (b) of 2017.

Fig. 8 Correlation between $PM_{2.5}$ concentrations of (a) OC (μg C m^{-3}) and levoglucosan (μg m^{-3}) and (b) K^+ and levoglucosan (μg m^{-3}) during winter and spring of 2017.

Fig. 9 Correlation between $PM_{2.5}$ concentrations of OC (μg C m^{-3}) and K^+ (μg m^{-3}) during winter (a) and spring (b) of 2017.

858 Fig. 10 Scatter plot of levoglucosan/K^+ versus levoglucosan/mannosan from different types of BB emissions, including those measured
859 in Ulaanbaatar (blue circles and red squares).
860 Fig. 11 Comparison of previously reported OC/levoglucosan ratios for softwood burning.
861 Fig. 12 Graphical determination of optimized OC/levoglucosan ratios used to estimate $PM_{2.5}$ concentrations of OC_{BB} in Ulaanbaatar in
862 winter (a) and spring (b) of 2017.
863 Fig. 13 Relative contributions (μg C m^{-3}) of OC_{BB} and $OC_{non\text{-}BB}$ to $PM_{2.5}$ in Ulaanbaatar during winter and spring of 2017.
864
865
866
867

868

869

870

871

872

873

874

875 Fig. 1

876

877

878

879
880

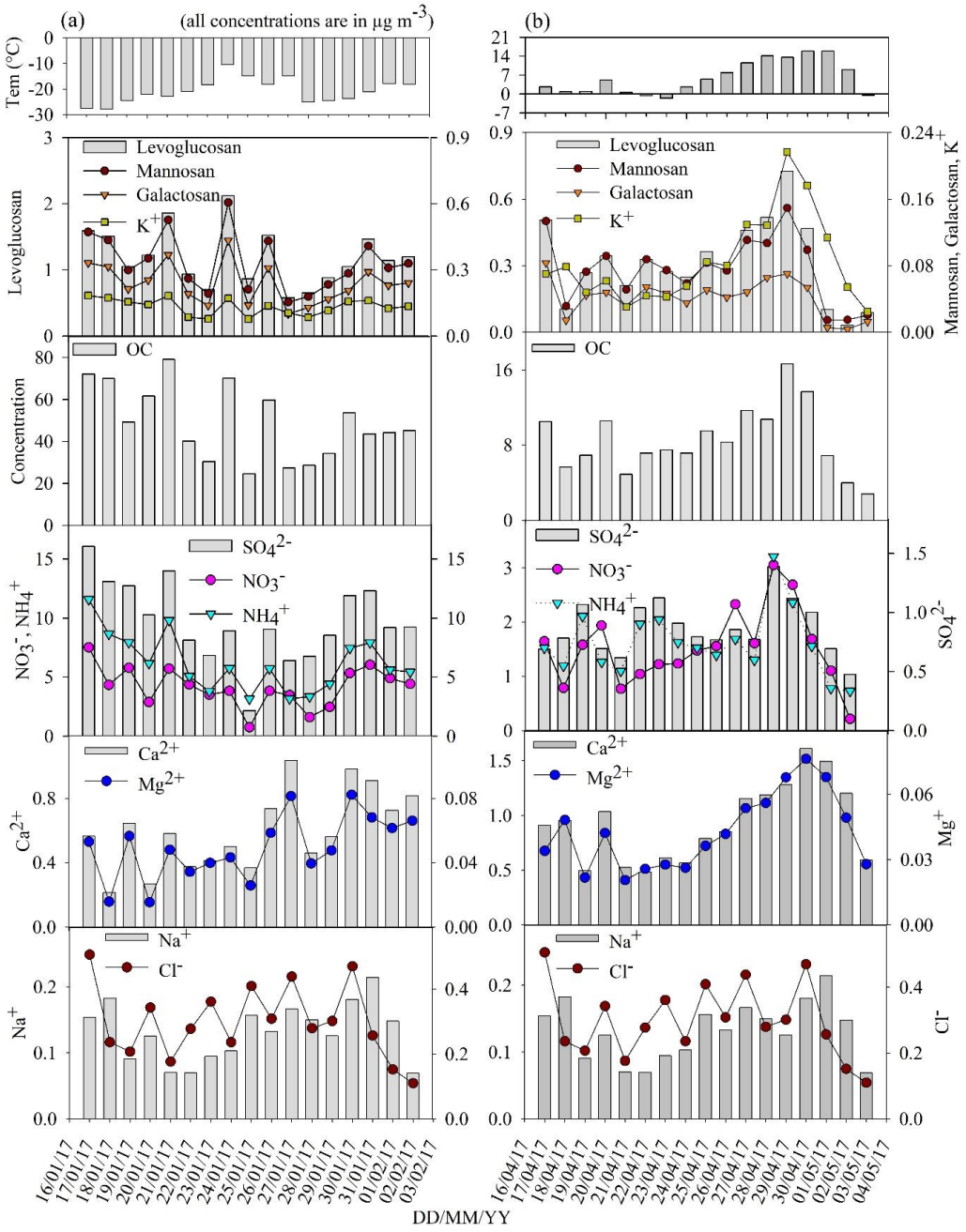

Fig. 2

881

882
883 Fig. 3
884
885
886

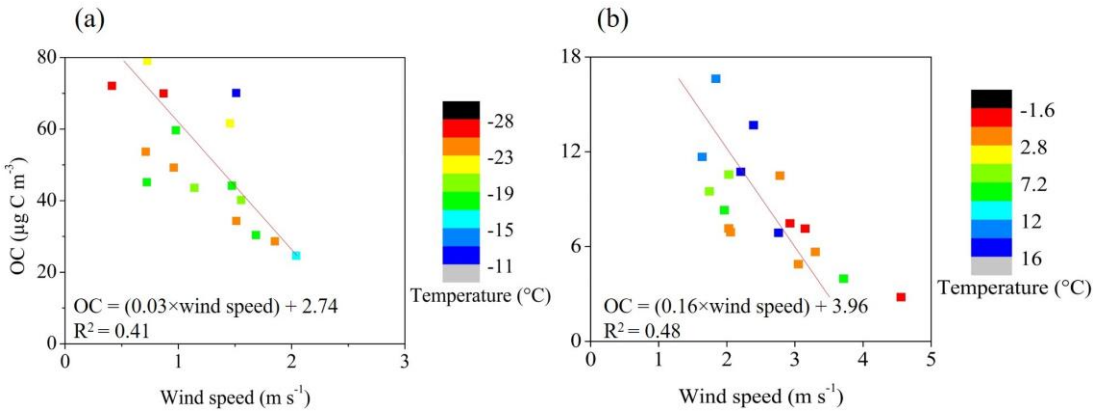

887
888
889

890 Fig. 4
891
892

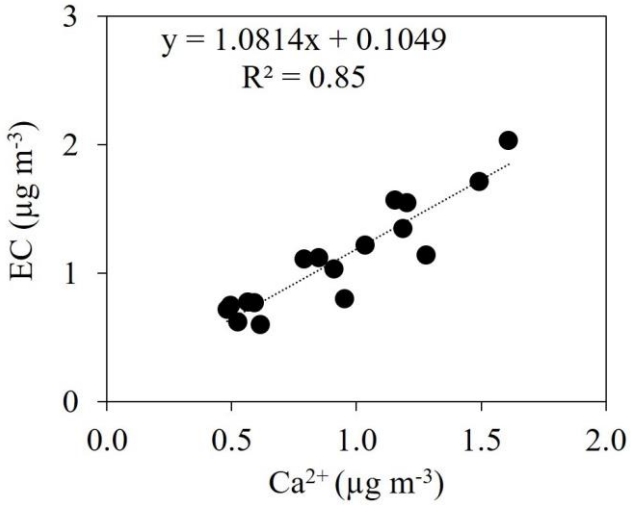

893
894
895

Fig. 5

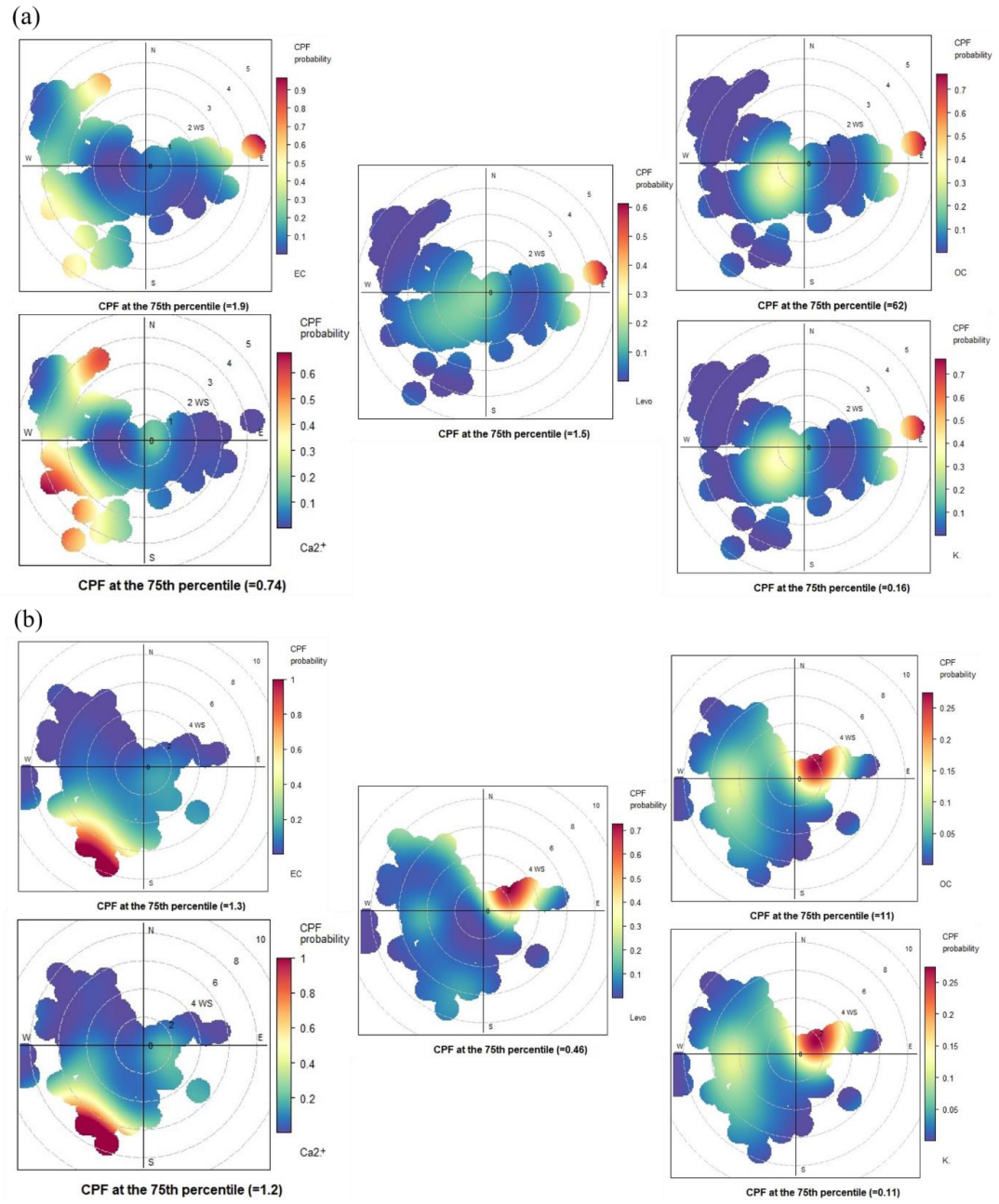
(a)
CPF probability
EC
CPF at the 75th percentile (=1.9)
Levo
CPF at the 75th percentile (=1.5)
OC
CPF at the 75th percentile (=62)
Ca2+
CPF at the 75th percentile (=0.74)
K
CPF at the 75th percentile (=0.16)
(b)
CPF at the 75th percentile (=1.3)
CPF at the 75th percentile (=0.46)
CPF at the 75th percentile (=11)
CPF at the 75th percentile (=1.2)
CPF at the 75th percentile (=0.11)

Fig. 6

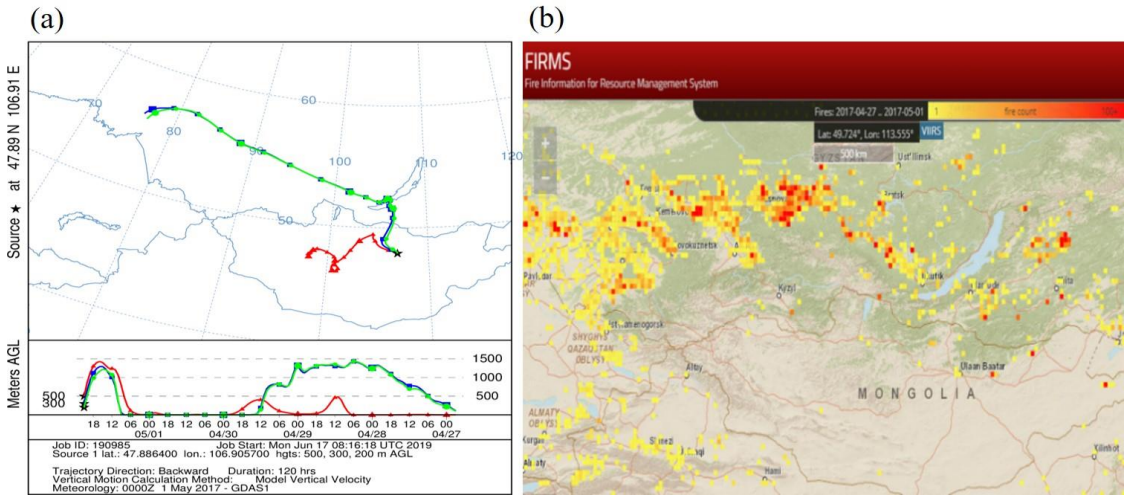
(a)
(b)
Source ★ at 47.89 N 106.91 E
Meters AGL
1500
1000
500
18 12 06 00 18 12 06 00 18 12 06 00 18 12 06 00 18 12 06 00
05/01 04/30 04/29 04/28 04/27
Job ID: 190985 Job Start: Mon Jun 17 08:16:18 UTC 2019
Source 1 lat.: 47.886400 lon.: 106.905700 hgts: 500, 300, 200 m AGL
Trajectory Direction: Backward Duration: 120 hrs
Vertical Motion Calculation Method: Model Vertical Velocity
Meteorology: 0000Z 1 May 2017 - GDAS1
FIRMS
Fire Information for Resource Management System
MONGOLIA

911 Fig. 7
912

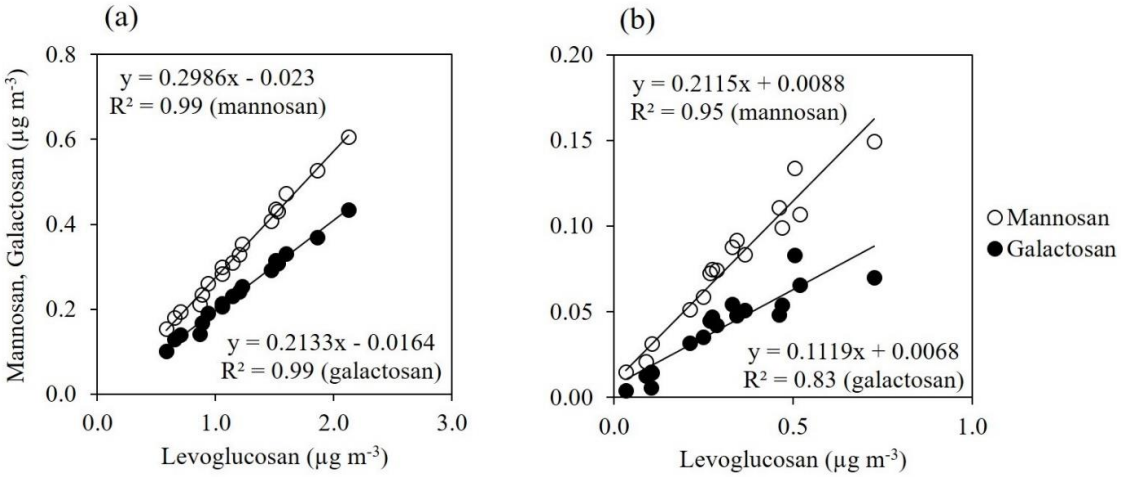

913
914

915 Fig. 8
916

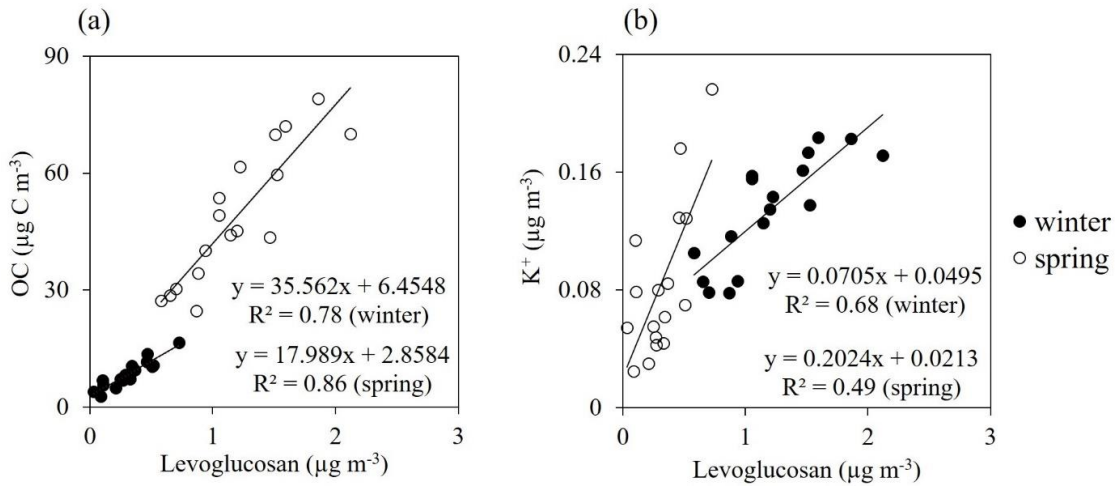

917
918

Fig. 9

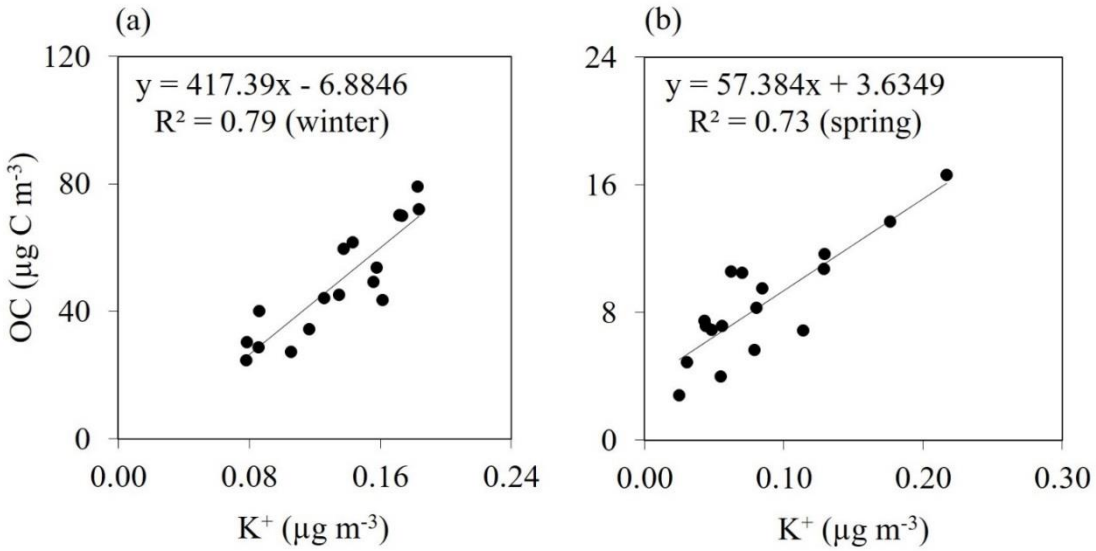
(a)
y = 417.39x - 6.8846
R² = 0.79 (winter)
OC (μg C m-3)
K+ (μg m-3)
(b)
y = 57.384x + 3.6349
R² = 0.73 (spring)
K+ (μg m-3)

923 Fig. 10
924

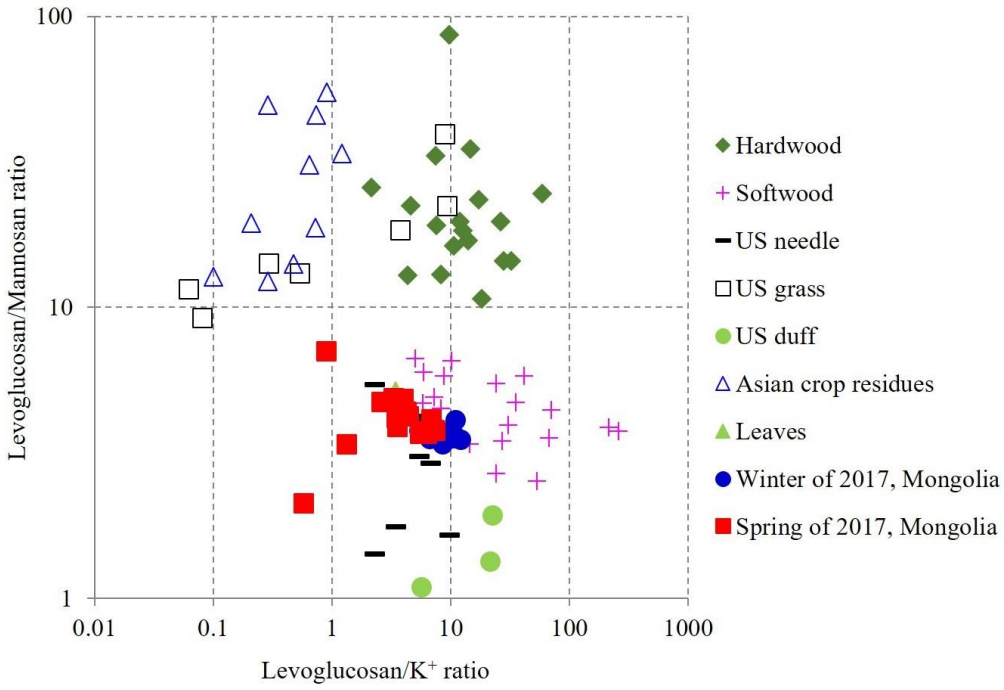

925
926

927 Fig. 11
928
929

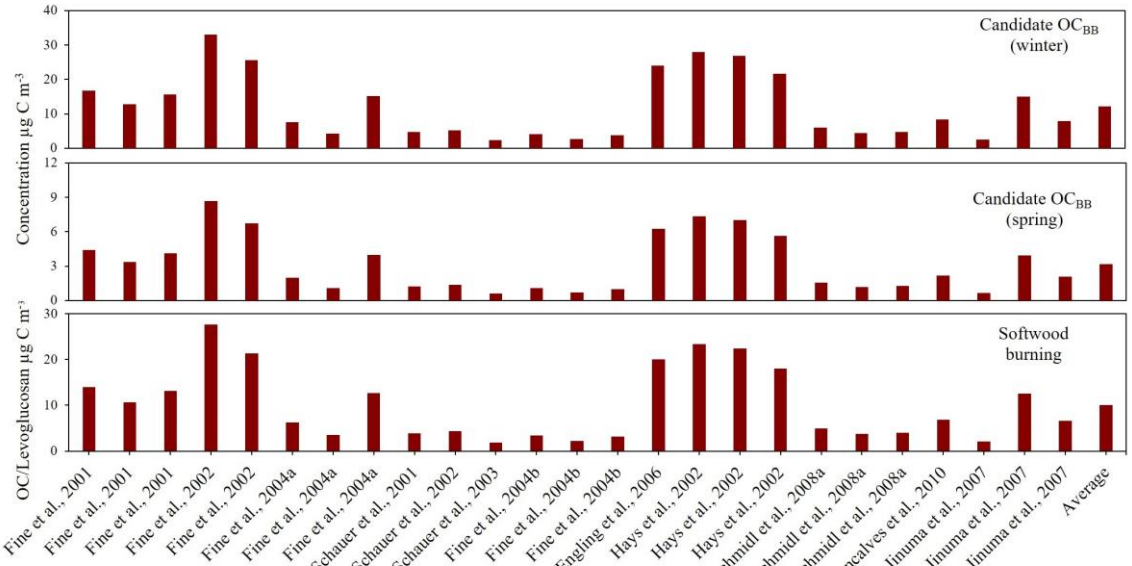

930
931
932

Fig. 12

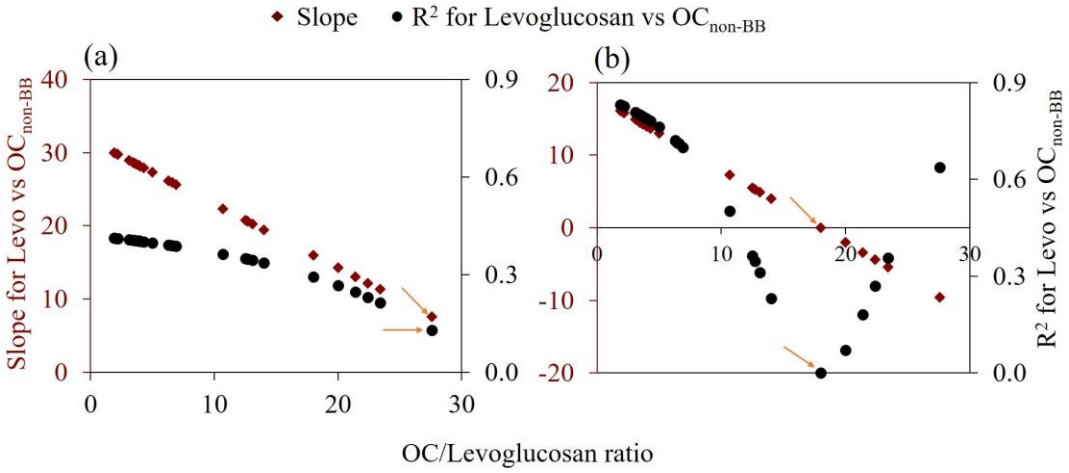
Slope
R² for Levoglucosan vs OC non-BB
(a)
(b)
Slope for Levo vs OC non-BB
R² for Levo vs OC non-BB
OC/Levoglucosan ratio

968 Fig. 13
969

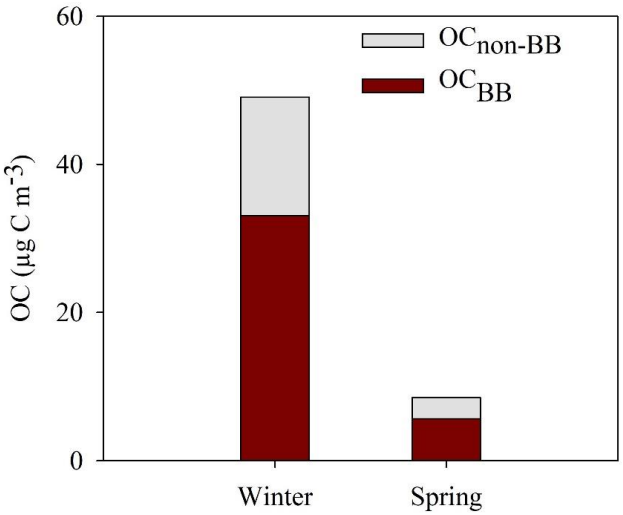

970
971
972